JCTC Journal of Chemical Theory and Computation

Long-Range-Corrected Hybrids Based on a New Model Exchange Hole

Elon Weintraub,† Thomas M. Henderson,* and Gustavo E. Scuseria

Department of Chemistry, Rice University, 6100 Main Street, Houston, Texas 77005-1892

Received December 3, 2008

Abstract: By admixing a fraction of exact Hartree−Fock-type exchange with conventional semilocal functionals, global hybrids greatly improve the accuracy of Kohn−Sham density functional theory. However, because global hybrids exhibit incorrect asymptotic decay of the exchange-correlation potential, they can have large errors for diverse quantities such as reaction barrier heights, nonlinear optical properties, and Rydberg and charge-transfer excitation energies. These errors can be removed by using a long-range-corrected hybrid, which uses exact exchange in the long range. Evaluating the long-range-corrected exchange energy requires a model for the semilocal exchange hole, and such models are scarce. Recently, two of us introduced one such model (*J. Chem. Phys.* **2008**, *128*, 194105). This model obeys several exact constraints and was designed specifically for use in long-range-corrected hybrids. Here, we give sample results for three long-range-corrected hybrids based upon our exchange hole model and show how the model can easily be applied to any generalized gradient approximation (GGA) for the exchange energy to create a long-range-corrected GGA.

1. Introduction

Due to its remarkable combination of accuracy and computational simplicity, Kohn−Sham (KS) density functional theory (DFT)[1,2] has become the predominant method in electronic structure calculations for molecules and solids.[3] The key ingredient in KS-DFT is the exchange-correlation functional, which accounts for many-body effects in a simple single-particle picture. Unfortunately, while many properties of the exact exchange-correlation functional are known, and (through the constrained search formalism)[4,5] even the precise form is available, a computationally tractable form is not.

Simple semilocal functionals, in which the exchange-correlation energy density at a point $\boldsymbol{r}$ depends only the density, its derivatives, and possibly the KS orbitals and their derivatives at $\boldsymbol{r}$, have been reasonably successful. The simplest (semi)local functional is the local density approximation (LDA), which takes the exchange-correlation energy density at a point with density n to be the exchange-correlation energy density of a homogeneous electron gas (HEG) with density n. More sophisticated generalized gradient approximations[6−10] (GGAs) and meta-GGAs[11−14] improve upon this basic form by adding information about the local density gradient (GGAs) and the local kinetic energy density or local density laplacian (meta-GGAs).

To reach the accuracy expected in molecular calculations, however, it is generally necessary to incorporate some fraction of nonlocal Hartree−Fock-type exchange. Usually, this is done by means of a global hybrid functional,[15−19] in which the exchange-correlation energy is written as

$$E_{\mathrm{xc}}^{\mathrm{GH}} = E_{\mathrm{xc}}^{\mathrm{DFA}} + c\left(E_{\mathrm{x}}^{\mathrm{HF}} - E_{\mathrm{x}}^{\mathrm{DFA}}\right) \tag{1}$$

Here, $E_{\mathrm{xc}}^{\mathrm{DFA}}$, $E_{\mathrm{x}}^{\mathrm{DFA}}$, and $E_{\mathrm{x}}^{\mathrm{HF}}$ are respectively some semilocal density functional approximation (DFA) to the exchange-correlation energy, a semilocal approximation to the exchange energy, and nonlocal Hartree−Fock (HF) exchange. The constant c controls the fraction of exact exchange included and usually varies between about 1/5 and 1/2. But while the simple global hybrid form is the most commonly used way of including some amount of HF-type exchange, much progress has been made over the past decade in

* Corresponding author e-mail: Thomas.Henderson@rice.edu.
† Permanent address: Rutgers University, New Brunswick, NJ 08901.

10.1021/ct800530u CCC: $40.75
Published on Web 03/20/2009

functionals with more flexible admixtures. One promising route is to use a range-separated fraction of exact exchange.[20−22] (Note that these works propose also to use a range-separated fraction of wave function correlation, which we here prefer to avoid.)

In a range-separated hybrid, the interelectronic Coulomb operator is generally decomposed into a long-range (LR) and a short-range (SR) part, typically as

$$\frac{1}{r_{12}} = \underbrace{\frac{\mathrm{erfc}(\omega r_{12})}{r_{12}}}_{\mathrm{SR}} + \underbrace{\frac{\mathrm{erf}(\omega r_{12})}{r_{12}}}_{\mathrm{LR}} \tag{2}$$

Different fractions of exact exchange are used in the two ranges. That is, the exchange-correlation energy of a range-separated hybrid can be written as

$$E_{\mathrm{xc}}^{\mathrm{RSH}} = E_{\mathrm{xc}}^{\mathrm{DFA}} + c_{\mathrm{SR}}(E_{\mathrm{x}}^{\mathrm{SR\text{-}HF}} - E_{\mathrm{x}}^{\mathrm{SR\text{-}DFA}}) + c_{\mathrm{LR}}(E_{\mathrm{x}}^{\mathrm{LR\text{-}HF}} - E_{\mathrm{x}}^{\mathrm{LR\text{-}DFA}}) \tag{3}$$

For applications to solids, in which the long-range HF-type exchange is both computationally and formally problematic,[23] we use a screened exchange which sets $c_{\mathrm{LR}} = 0$.[24−27] In finite systems, long-range HF-type exchange is the exact long-range exchange-correlation functional, unless long-range correlations (such as might be found, for instance, in dissociation on the symmetry-restricted surface) are present. It is therefore common in finite systems to set $c_{\mathrm{LR}} = 1$ and $c_{\mathrm{SR}} = 0$.[28−33] Functionals which use 100% long-range HF-type exchange are termed long-range-corrected hybrids. Long-range-corrected hybrids dramatically improve upon global hybrids in the description of charge transfer and Rydberg excitations,[29,34] nonlinear optical properties,[28,35] reaction barrier heights,[30−32] and so on. The two limits of screened and long-range-corrected functionals can be reconciled by using exact exchange in the *middle* range, as in the recently proposed functional of Henderson et al.[36,37]

To define the long-range or short-range semilocal exchange energy, we require a semilocal model for the exchange hole. While many semilocal functionals are constructed from such a model, many others are not. Most range-separated hybrids of GGAs have used one of two models: the LDA-based model of Iikura and co-workers[28] (ITYH) or the model of Ernzerhof and Perdew[38] (EP). The ITYH model is quite flexible and can readily be applied to any GGA or meta-GGA. The EP model was parametrized to reproduce the GGA of Perdew et al.[9] (PBE), and while it could be reparameterized to fit other GGAs, this has not, to the best of our knowledge, been done.

Recently, two of us proposed a new GGA model, based on that of EP, but constructed specifically for use in range-separated hybrids.[39] This new exchange hole model (here denoted HJS) follows the EP model in satisfying more exact constraints than does the model of ITYH, but differs from the EP model in that the range-separated exchange energy density can be evaluated analytically.

In this work, we examine the performance of three long-range-corrected hybrid functionals based on our newer exchange hole model. Let us be clear at the outset that our intention is not to provide a thorough benchmarking of new long-range-corrected hybrids. Rather, it is to show how, by modifying a few parameters in the HJS hole model, one can construct long-range-corrected hybrids of various GGAs, affording much (but not all) of the flexibility inherent in the approach of ITYH while avoiding some of its weaknesses (see ref 39).

Section 2 of this paper briefly describes the HJS model exchange hole, while in section 3 we remind the reader of the form of the exchange functionals considered here. Section 4 presents the results of long-range-corrected hybrids based on those GGAs, and general conclusions are drawn in section 5. Appendix A provides a numerically stable expression for the short-range exchange energy coming from the HJS model exchange hole.

2. HJS Model Exchange Hole

The HJS model exchange hole is given by

$$\mathscr{T}(s,y) = \left[\left(\frac{9}{4}\frac{\mathscr{A}}{y^2} + \mathscr{B} + \mathscr{C}\mathscr{F}(s)y^2 + \mathscr{E}\mathscr{G}(s)y^4\right)\mathrm{e}^{-\mathscr{D}y^2} - \frac{9}{4y^4}(1 - \mathrm{e}^{-\mathscr{A}y^2})\right]\mathrm{e}^{-s^2\mathscr{H}(s)y^2} \tag{4}$$

where

$$y = k_{\mathrm{F}} r_{12} \tag{5a}$$

$$s = \frac{|\nabla n|}{2k_{\mathrm{F}} n} \tag{5b}$$

$$k_{\mathrm{F}} = (3\pi^2 n)^{1/3} \tag{5c}$$

The exchange hole for σ-spin electrons can readily be obtained by replacing the total density n with the density of σ-spin electrons n_σ, and writing $k_{\mathrm{F},\sigma} = (6\pi^2 n_\sigma)^{1/3}$.

The parameters $\mathscr{A}$, $\mathscr{B}$, $\mathscr{C}$, $\mathscr{D}$, and $\mathscr{E}$ are chosen so that, at $s = 0$, the HJS model exchange hole reduces to a nonoscillating approximation to the LDA exchange hole, with proper value and curvature at $y = 0$, proper energy and normalization, and minimal oscillation. Numerical values to six digits are $\mathscr{A} = 0.757211$, $\mathscr{B} = -0.106364$, $\mathscr{C} = -0.118649$, $\mathscr{D} = 0.609650$, and $\mathscr{E} = -0.0477963$. (Note that $\mathscr{B}$, $\mathscr{C}$, and $\mathscr{E}$ are defined in terms of $\mathscr{A}$ and $\mathscr{D}$, and so are defined to more decimal places; see ref 39 for the equations relating the various parameters.)

The function $\mathscr{G}(s)$ is chosen to enforce normalization for nonzero gradients, while $\mathscr{F}(s)$ enforces proper curvature at $y = 0$ for small gradients, and is restricted such that it remains bounded. These functions take the form

$$\mathscr{F}(s) = 1 - \frac{1}{27\mathscr{C}}\frac{s^2}{1 + s^2/s_0^2} - \frac{1}{2\mathscr{C}}s^2\mathscr{H}(s) \tag{6a}$$

$$\mathscr{E}\mathscr{G}(s) = -\frac{2}{5}\mathscr{C}\mathscr{F}(s)\lambda - \frac{4}{15}\mathscr{B}\lambda^2 - \frac{6}{5}\mathscr{A}\lambda^3 - \frac{4}{5}\sqrt{\pi}\lambda^{7/2} - \frac{12}{5}\lambda^{7/2}(\sqrt{\zeta} - \sqrt{\eta}) \tag{6b}$$

where $s_0 = 2$, and where we have defined

$$\zeta = s^2\mathscr{H}(s) \tag{7a}$$

$$\eta = \mathscr{A} + s^2\mathscr{H}(s) = \mathscr{A} + \zeta \tag{7b}$$

$$\lambda = \mathscr{D} + s^2\mathscr{H}(s) = \mathscr{D} + \zeta \tag{7c}$$

Finally, the function $\mathscr{H}(s)$ is chosen so that the HJS model exchange hole gives the desired exchange energy. The ratio of the GGA exchange energy density to the LDA exchange energy density is termed the enhancement factor:

$$F_x = \frac{\epsilon_x^{GGA}}{\epsilon_x^{LDA}} \tag{8}$$

For a GGA, F_x depends only the reduced gradient s. In terms of the model exchange hole, it is given by

$$F_x(s) = -\frac{8}{9}\int_0^\infty dy\, y\mathscr{T}(s,y) \tag{9a}$$

$$= \mathscr{A} - \frac{4}{9}\frac{\mathscr{B}}{\lambda} - \frac{4}{9}\frac{\mathscr{C}\mathscr{F}(s)}{\lambda^2} - \frac{8}{9}\frac{\mathscr{E}\mathscr{G}(s)}{\lambda^3} + \zeta\ln\left(\frac{\zeta}{\lambda}\right) - \eta\ln\left(\frac{\eta}{\lambda}\right) \tag{9b}$$

Given a GGA (and thus an enhancement factor), we solve the foregoing equation numerically for $\mathscr{H}(s)$ over a range of values of s and fit the resulting curve to

$$\mathscr{H}(s) = (a_2s^2 + a_3s^3 + a_4s^4 + a_5s^5 + a_6s^6 + a_7s^7)/(1 + b_1s + b_2s^2 + b_3s^3 + b_4s^4 + b_5s^5 + b_6s^6 + b_7s^7 + b_8s^8 + b_9s^9) \tag{10}$$

constraining this rational function to have the correct small s and large s expansion when possible. [Usually, this means fixing a_2 to give the second-order gradient expansion coefficient from the target enhancement factor, setting $a_3 = a_2b_1$ to eliminate the third-order gradient expansion coefficient, and writing $a_7 = ab_9$, $a_6 = ab_8$, and $a_5 = ab_7 + bb_9$, where a is chosen so that the $s\rightarrow\infty$ limit of the enhancement factor is the correct constant, and b is chosen so that the next term in the asymptotic expansion of $F_x(s)$ is also correct.]

Once we have defined $\mathscr{H}(s)$, we use our model exchange hole to define the range-separated enhancement factor. Most commonly, we use

$$V_{ee}^{SR} = \frac{\mathrm{erfc}(\omega r_{12})}{r_{12}} \tag{11}$$

in which case the range-separated enhancement factor is given by

$$F_x^{SR}(s,\nu) = -\frac{8}{9}\int_0^\infty dy\, y^2\frac{\mathrm{erfc}(\nu y)}{y}\mathscr{T}(s,y) \tag{12}$$

where $\nu = \omega/k_F$. This integral can be evaluated explicitly, and the result is

$$F_x^{SR}(s,\nu) = \mathscr{A} - \frac{4}{9}\frac{\mathscr{B}}{\lambda}(1-\chi) - \frac{4}{9}\frac{\mathscr{C}\mathscr{F}(s)}{\lambda^2}\left(1 - \frac{3}{2}\chi + \frac{1}{2}\chi^3\right) - \frac{8}{9}\frac{\mathscr{E}\mathscr{G}(s)}{\lambda^3}\left(1 - \frac{15}{8}\chi + \frac{5}{4}\chi^3 - \frac{3}{8}\chi^5\right) + 2\nu\left(\sqrt{\zeta+\nu^2} - \sqrt{\eta+\nu^2}\right) + 2\zeta\ln\left(\frac{\nu+\sqrt{\zeta+\nu^2}}{\nu+\sqrt{\lambda+\nu^2}}\right) - 2\eta\ln\left(\frac{\nu+\sqrt{\eta+\nu^2}}{\nu+\sqrt{\lambda+\nu^2}}\right) \tag{13}$$

where

$$\chi = \frac{\nu}{\sqrt{\lambda+\nu^2}} \tag{14}$$

Evaluating this expression for large ν is fraught with numerical problems; see Appendix A for an analytic simplification which allows more robust evaluation of the enhancement factor.

3. Three Prototype Exchange Functionals

We do not wish here to provide an exhaustive survey of long-range-corrected hybrids based on various combinations of semilocal exchange and semilocal correlation functionals. Instead, we wish to consider three functionals in particular: the PBE GGA of Perdew, Burke, and Ernzerhof,[9] the PBEsol functional of Perdew and co-workers,[10] and the BLYP combination of Becke's 1988 exchange functional[6] and the correlation functional of Lee, Yang, and Parr.[7] While PBE provides a reasonably balanced description of finite systems and solids, PBEsol is geared principally for applications to solids, and BLYP is more successful for atoms and molecules. The three functionals thus provide prototype cases for us. The parameters defining $\mathscr{H}(s)$ for each are listed in Table 1. Note that we show the coefficients of powers of $s_\sigma = |\nabla n_\sigma|/(2(6\pi^2)^{1/3}n_\sigma^{4/3})$.

3.1. PBE and PBEsol. The PBE exchange enhancement factor can be written as

$$F_x^{PBE} = 1 + \kappa\frac{\mu s^2}{\kappa + \mu s^2} \tag{15}$$

where $\kappa = 0.804$ enforces the local Lieb−Oxford bound, and $\mu \approx 0.2195$ controls the small gradient behavior, which for the foregoing functional form is

$$F_x^{PBE} = 1 + \mu s^2 + ... \tag{16}$$

The exact small gradient expansion turns out to be[40]

$$F_x = 1 + \frac{10}{81}s^2 + ... \approx 1 + 0.1235s^2 + ... \tag{17}$$

so PBE responds too strongly to small fluctuations in the density. This is intentional—the gradient expansion of the PBE *correlation* functional is correct, and the exact gradient response of the PBE exchange functional is sacrificed so that the linear response of the PBE exchange-correlation functional is the same as that of the LSDA.

Unfortunately, the overly large value of the second-order gradient coefficient in F_x causes problems in solids, in which

Table 1. Parameters in the Rational Functions Defining $H(s)$ for Various GGAs

	PBE	PBEsol	B88
a_2	0.015 9941	0.004 7333	0.025 3933
a_3	0.085 2995	0.040 3304	−0.067 3075
a_4	−0.160 368	−0.057 4615	0.089 1476
a_5	0.152 645	0.043 5395	−0.045 4168
a_6	−0.097 1263	−0.021 6251	−0.007 6581
a_7	0.042 2061	0.006 3721	0.014 2506
b_1	5.333 19	8.520 56	−2.650 60
b_2	−12.478 0	−13.988 5	3.911 08
b_3	11.098 8	9.285 83	−3.315 09
b_4	−5.110 13	−3.272 87	1.544 85
b_5	1.714 68	0.843 499	−0.198 386
b_6	−0.610 380	−0.235 543	−0.136 112
b_7	0.307 555	0.084 7074	0.064 7862
b_8	−0.077 0547	−0.017 1561	0.015 9586
b_9	0.033 4840	0.005 0552	$-2.450\,66 \times 10^{-4}$

for many properties, PBE offers little improvement over LDA. To remedy this, PBEsol takes the PBE form, but enforces the exact gradient expansion for exchange instead of for correlation. Accordingly, the PBEsol exchange enhancement factor is

$$F_{\mathrm{x}}^{\mathrm{PBEsol}} = 1 + \kappa\frac{\bar{\mu}s^2}{\kappa + \bar{\mu}s^2} \tag{18}$$

with $\bar{\mu} = 10/81$. The corresponding PBEsol correlation functional sacrifices the exact gradient expansion for correlation, and is chosen to provide a best fit to jellium surface energies (really, to jellium surface energies as predicted by the TPSS meta-GGA). The resulting functional performs more like LDA than does PBE, and performance improves for solids but degrades for molecules.

3.2. BLYP. In finite systems, the exchange energy density should asymptotically behave as $-\rho/r$, essentially so that the self-Coulomb repulsion of electrons in density tails can cancel with their self-exchange. Neither PBE nor PBEsol satisfies this constraint. It can, however, be enforced in the GGA framework. The B88 exchange functional does so by writing the enhancement factor for σ-spin electrons as

$$F_{\mathrm{x}}^{\mathrm{B88}} = 1 + \frac{1}{C_{\mathrm{x}}}\frac{\beta x_\sigma^{\,2}}{1 + 6\beta x_\sigma \sinh^{-1}(x_\sigma)} \tag{19}$$

Here, we have defined

$$x_\sigma = \frac{|\nabla n_\sigma|}{n_\sigma^{4/3}} = 2(6\pi^2)^{1/3}s_\sigma \tag{20a}$$

$$C_{\mathrm{x}} = \frac{3}{4\pi}(6\pi^2)^{1/3} \tag{20b}$$

$$\beta = 0.0042 \tag{20c}$$

The functional form of eq 19 guarantees the proper decay of the exchange energy density (but not the exchange potential) for exponentially decaying densities, though for large gradients the enhancement factor is not bounded.

Because the B88 enhancement factor is unbounded, the functional form we have chosen for $\mathscr{H}(s)$ is not asymptotically correct. We note from eq 10 that $s^2\mathscr{H}(s)$ goes to a finite limiting value as s goes to infinity. With bounded $s^2\mathscr{H}(s)$, we have bounded $\mathscr{F}(s)$, hence bounded $\mathscr{G}(s)$, and hence a bounded enhancement factor, $F_{\mathrm{x}}(s)$. In fact, near $s = 70$, our best fit to $\mathscr{H}(s)$ has a pole, and, for larger s, $\mathscr{H}(s)$ is negative and the enhancement factor acquires an imaginary part.

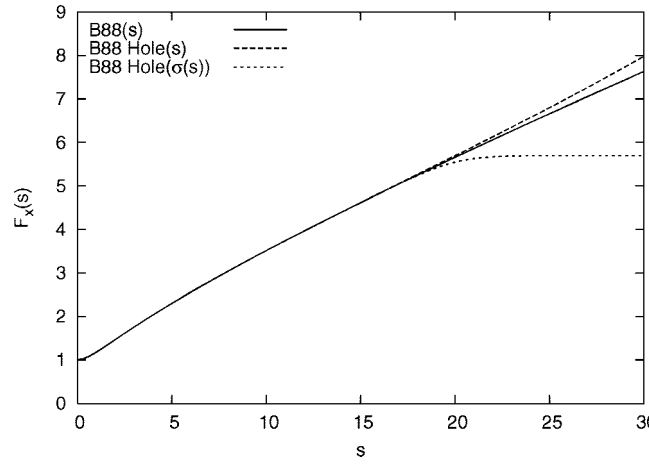

Figure 1. Exchange enhancement factors for the B88 functional, our exchange hole model to it, and the exchange hole model incorporating $\sigma(s)$.

Since we do not wish to change the functional form of $\mathscr{H}(s)$ in our model exchange hole, we are forced to do something about the large s behavior. We choose to modify the dimensionless density gradient, replacing s with $\sigma(s)$ in our code for the B88 exchange hole, with

$$\sigma(s) = -\ln\left(\frac{\mathrm{e}^{-s} + \xi}{1 + \xi}\right) \tag{21}$$

$$\xi = \frac{1}{\mathrm{e}^{20} - 1} \tag{22}$$

For small s, $\sigma(s) \approx s$, while, for large s, $\sigma(s)$ approaches 20. In doing so, we keep a reasonable fit to the exact B88 enhancement factor for $s \lesssim 20$, but the enhancement factor from our exchange hole model is bounded as s goes to infinity. Since the discrepancies between the B88 enhancement factor and that from our exchange hole model occur only at quite large s, we do not anticipate any significant energetic effects. Figure 1 shows the B88 enhancement factor, the enhancement factor from our exchange hole model, and the enhancement factor from our exchange hole model with $\sigma(s)$ used in place of s. As we shall see shortly, the energetic effects of cutting off the reduced gradient at $s = 20$ are negligible.

Note that we have reparametrized $\mathscr{H}(s)$ for our B88 hole model to improve agreement with the B88 enhancement factor for small gradients.

4. Results

In this section, we show results for long-range-corrected hybrids of the GGAs listed earlier. We also include a long-range-corrected LDA based on the $s = 0$ limit of the HJS exchange hole. For each functional considered, we optimize the parameter ω of eq 2 against the AE6 set of heats of

Table 2. Mean and Mean Absolute Errors for the AE6 Set of Atomization Energies, BH6 Set of Barrier Heights, and the Total Atomic Energies of H−Ar, Comparing GGAs (PBE, PBEsol, and BLYP) to Functionals Obtained from GGA Hole Models (EP PBE Hole, HJS PBE Hole, PBEsol Hole, and BLYP Hole)[a]

	AE6		BH6		atoms	
method	ME	MAE	ME	MAE	ME	MAE
LDA	76.96	76.96	−18.05	18.05	67.78	67.78
LDA hole	76.96	76.96	−18.05	18.05	67.78	67.78
PBEsol	35.40	35.40	−12.99	12.99	40.09	40.09
PBEsol hole	35.39	35.39	−12.99	12.99	40.09	40.09
PBE	11.89	15.14	−9.57	9.57	8.55	8.55
HJS PBE hole	11.88	15.13	−9.57	9.57	8.55	8.55
EP PBE hole	9.75	13.23	−9.41	9.41	7.21	7.24
BLYP	−1.96	6.88	−8.03	8.03	−0.56	1.21
BLYP hole	−1.94	6.88	−8.04	8.04	−0.56	1.21

[a] Results are in kilocalories per mole (AE6, BH6) or mH/electron (atomic total energies). We include LDA and the LDA limit of our hole model for comparison. Results are reported to two decimal places because it is only at this level that discrepancies between our exchange hole models and their parent semilocal functionals can be seen.

formation[41] and the BH6 set of barrier heights.[41] We then examine errors for the G1,[42,43] G2,[44] and G3[45] sets of heats of formation, the HTBH38[46] and NHTBH38[47] sets of reaction barriers, and the total atomic energies of H−Ar.[48] Throughout this work, we use the 6-311++G(3df,3pd) basis set and define errors as theory − experiment.

Before we examine long-range-corrected hybrids, however, we validate our parametrizations of the exchange holes by comparing, for several test sets, the results from the GGAs we consider to the results from our exchange holes. Table 2 shows the mean errors (ME) and mean absolute errors (MAE) for the AE6 set, the BH6 set, and the total atomic energies of H−Ar. We also include LDA and the results from the PBE hole model of Ernzerhof and Perdew.

As Table 2 makes clear, the PBE hole model of Ernzerhof and Perdew does not quite reproduce the PBE exchange energy, but actually gives results superior to those of PBE. This may explain some small portion of the accuracy of range-separated hybrids based upon it (because the values for very large or very small ω are more accurate than are those from PBE itself). The HJS version of the PBE hole more precisely reproduces the PBE results, and thus its thermochemical performance is slightly worse than that of the EP hole model. This can be expected to carry over to range-separated hybrids as well.

Table 2 also verifies that, as expected, PBEsol is intermediate in quality between LDA and PBE. Finally, we see that BLYP significantly outperforms the other two GGAs for thermochemistry and that cutting off the reduced gradient at $s = 20$ indeed has no significant effect.

4.1. Optimizing ω for Long-Range-Corrected Hybrids. To optimize the value of ω for the long-range-corrected hybrids under consideration, we minimize the mean absolute error in the AE6 set of atomization energies and the BH6 set of barrier heights. Since, for the very successful long-range-corrected LC-ωPBE hybrid of Vydrov and Scuseria,[31] the errors in atomization energies are roughly three times as large as the errors in barrier heights, we weight barrier heights as three times as important as atomization energies in choosing ω. We use LC-ωPBE orbitals in this portion of the work; our experience shows that self-consistency makes only a small difference. Figures 2−4 show the MAE in kilocalories per mole for the AE6 and BH6 sets as a function of ω, as well as the MAE in milliHartree per electron for the total energies of H−Ar. Note the significant difference in scale on the three figures. All three figures include results for "PBE", which signifies what we shall term LC-ωPBE08 and by which we mean a version of LC-ωPBE based on the HJS exchange hole.

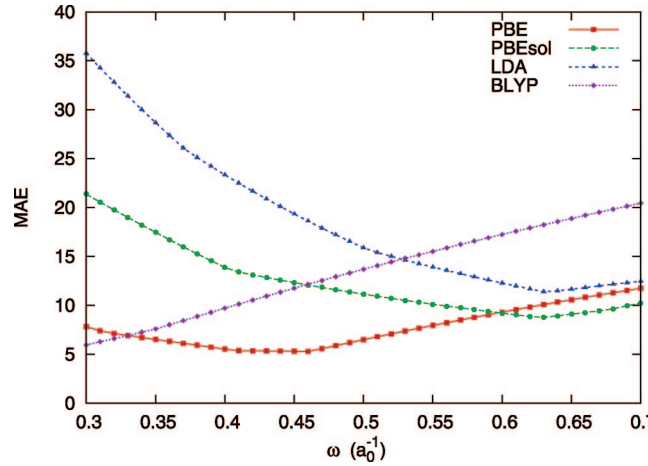

Figure 2. Mean absolute errors in the AE6 set (kcal/mol) from the LC-ωPBE08, LC-ωPBEsol, LC-ωLDA, and LC-ωBLYP functionals as a function of ω.

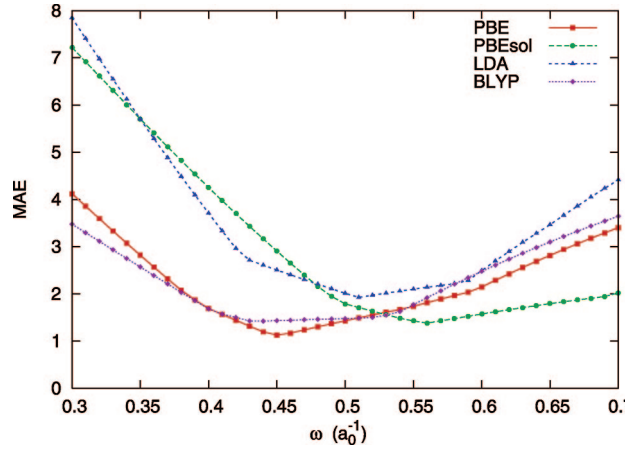

Figure 3. Mean absolute errors in the BH6 set (kcal/mol) from the LC-ωPBE08, LC-ωPBEsol, LC-ωLDA, and LC-ωBLYP functionals as a function of ω.

We begin with a few general comments before turning to the individual GGAs. Performance for thermochemistry is very strongly functional-dependent. Indeed, while LC-ωLDA, LC-ωPBEsol, and LC-ωPBE08 show a minimum in the error as a function of ω, LC-ωBLYP does not, at least in the range considered here. The optimal value of ω appears to increase as the functional becomes more like LDA. Note in this context that even the best results for LC-ωPBEsol and LC-ωLDA yield errors on the order of 10−15 kcal/mol. Barrier heights, by contrast, all show minima in the range of ω considered, and over a fairly narrow range at that. Note also that the best results for barrier heights are consistently

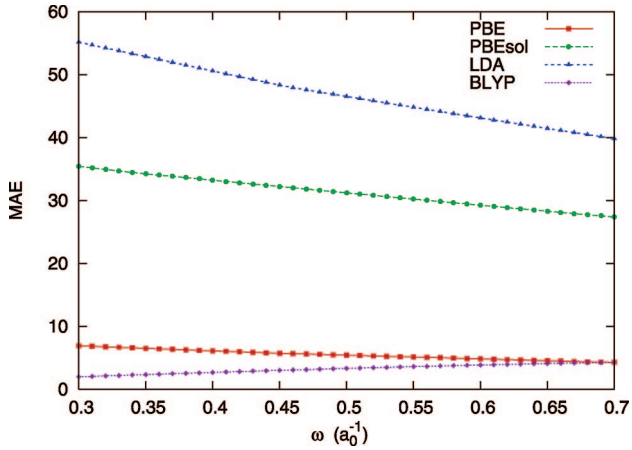

Figure 4. Mean absolute errors in the atomic total energies of H−Ar (mH/electron) from the LC-ωPBE08, LC-ωPBEsol, LC-ωLDA, and LC-ωBLYP functionals as a function of ω.

in the range of 1−3 kcal/mol. We are less interested in atomic total energies but wish to remind the reader of the characteristically large errors in LDA-based hybrids and to point out that these errors are also observed in LC-ωLDA and LC-ωPBEsol.

We now turn to the selection of ω for the various long-range-corrected hybrids under consideration, beginning with PBE. Since the differences between the EP and HJS hole models for PBE are rather small, we do not expect significant differences between LC-ωPBE and what we shall term LC-ωPBE08. We also expect the value of ω in LC-ωPBE08 to be similar to the value used in LC-ωPBE ($\omega = 0.40a_0^{-1}$, where a_0 is the Bohr radius). In fact, the optimal value for LC-ωPBE08 is, by our criterion, $\omega = 0.45a_0^{-1}$. As can be seen from Figures 2 and 3, this value essentially optimizes the barrier heights, as errors in atomization energy are rather flat near this value.

Before considering PBEsol, we turn to LC-ωLDA. We should emphasize here that, by LC-ωLDA, we mean a long-range-corrected functional based on the zero-gradient limit of the HJS exchange hole (which is a nonoscillating approximation to the true LDA exchange hole). Results are thus expected to be similar to, but not identical to, previous results using a long-range-corrected LDA. Figures 2 and 3 show that, unlike with LC-ωPBE08, the minima for the AE6 and BH6 sets as a function of ω do not overlap particularly well. While barrier heights are optimized with $\omega \approx 0.5a_0^{-1}$, atomization energies prefer $\omega \approx 0.6a_0^{-1} - 0.65a_0^{-1}$. This is in qualitative agreement with the results of ref 49, which finds that the optimal value of ω for long-range-corrected LDA is smaller for barrier heights than it is for thermochemistry. Our criterion selects $\omega = 0.60a_0^{-1}$, essentially because barrier heights are rather less sensitive to the precise value of ω than are atomization energies, at least in the range under consideration.

Since PBEsol is intermediate between PBE and LDA, we expect the value of ω to be between that used in LC-ωPBE and the optimal value in a long-range-corrected LDA. From Figure 2, it is clear that LC-ωPBEsol does not perform as well for thermochemistry as does LC-ωPBE, and the thermochemically optimal ω is essentially the same as for LC-ωLDA. But LC-ωPBEsol performs almost as well as does LC-ωPBE for barrier heights, though the value of ω needed is rather larger. We select $\omega = 0.60a_0^{-1}$ for the functional, though any value between $0.55a_0^{-1}$ and $0.65a_0^{-1}$ would do.

Table 3. Errors in Thermochemistry for Several Long-Range-Corrected GGAs and for Their Parent GGAs[a]

	G1		G2		G3		atoms	
model	ME	MAE	ME	MAE	ME	MAE	ME	MAE
LDA	−36.2	36.2	−83.3	83.3	−121.5	121.5	67.8	67.8
PBEsol	−16.9	17.2	−40.7	40.9	−58.7	58.8	40.1	40.1
PBE	−6.7	8.2	−16.1	16.9	−21.7	22.2	8.6	8.6
BLYP	−2.9	4.8	−0.6	7.3	3.8	9.5	−0.6	1.2
LC-ωLDA	−2.3	8.4	−6.2	12.0	−8.4	14.6	39.9	42.9
LC-ωPBEsol	1.5	5.5	−5.1	9.5	−9.9	13.6	28.5	29.2
LC-ωPBE	2.1	3.5	−0.4	3.7	−0.9	4.2	4.4	5.0
LC-ωPBE08	2.8	3.9	0.0	3.9	−1.1	4.7	5.0	5.7
LC-ωBLYP	3.1	4.5	7.8	8.3	13.1	13.5	−2.6	2.7

[a] We show mean errors (ME) and mean absolute errors (MAE) in kilocalories per mole for the G1, G2, and G3 sets of heats of formation, and in mH/electron for the total atomic energies of H−Ar.

Finally, since B88 is in some sense "farther" from LDA than is PBE, we might expect the optimal value of ω for LC-ωBLYP to be somewhat lower than the $0.45a_0^{-1}$ used in LC-ωPBE08. As Figures 2 and 3 establish, this is indeed the case. While there is a broad minimum in the error for barrier heights, the error for atomization energies strictly increases as a function of ω in the region considered. We choose $\omega = 0.40a_0^{-1}$ as a compromise between accuracy for reaction barriers and that for atomization energies, though a slightly smaller value would also suffice.

With these optimized values for ω, we use self-consistent orbitals in what follows. Note that optimization using self-consistent orbitals and larger test sets could lead to slightly different choices of ω, as could weighting atomization energies differently relative to barrier heights. Throughout, we use the procedures described in ref 50.

4.2. Thermochemistry. Performance for thermochemistry can be examined somewhat more thoroughly by calculating the heats of formation for the molecules in the G1, G2, and G3 sets. Because the G2 (G3) set is a superset of the G1 (G2) set which primarily adds larger molecules, we can identify size-dependent errors by examining the relative performance for the three sets. Results are shown in Table 3. We also include results for total atomic energies, since it is known that, by adjusting the atomic energies, one can dramatically improve heats of formation.[51]

As might be expected, LC-ωPBE08 does not perform much differently than does LC-ωPBE. Since we have already seen that the EP PBE hole model gives slightly better thermochemistry than does PBE, it is not terribly surprising that LC-ωPBE08 is slightly inferior to LC-ωPBE. Nonetheless, results from LC-ωPBE08 are quite reasonable, and it is reassuring to note that the small differences between the EP and HJS model exchange holes have only small effects on the accuracy of long-range-corrected hybrids.

The success of LC-ωPBE is already well-documented, and it is not our intent to belabor the point, even with a slightly different hole model. But we do wish to point out that there

Table 4. Errors in Barrier Heights for Several Long-Range-Corrected GGAs and for Their Parent GGAs[a]

	HTBH38		NHTBH38	
model	ME	MAE	ME	MAE
LDA	−17.9	17.9	−12.4	12.7
PBEsol	−13.1	13.1	−9.9	10.1
PBE	−9.7	9.7	−8.5	8.6
BLYP	−7.8	7.8	−8.7	8.7
LC-ωLDA	3.7	4.2	5.6	5.8
LC-ωPBEsol	1.3	2.1	4.1	4.4
LC-ωPBE	−0.5	1.3	1.4	2.4
LC-ωPBE08	0.4	1.4	2.5	2.9
LC-ωBLYP	0.0	2.2	0.5	1.8

[a] We show mean errors (ME) and mean absolute errors (MAE) in kcal/mol for the HTBH38 and NHTBH38 sets of reaction barriers.

is something rather special about the PBE GGA; other long-range-corrected hybrids based on the same hole model but parametrized to reproduce different GGAs are noticeably inferior. That LC-ωPBEsol is not as accurate for thermochemistry as is LC-ωPBE is unsurprising, since LC-ωLDA is less accurate than is LC-ωPBE. We see large size-dependent errors in LC-ωPBEsol and LC-ωLDA, which is not terribly surprising since the atomic total energies are very poor. Interestingly, the size effects in LC-ωLDA are noticeably weaker than are those in LC-ωPBEsol.

Surprisingly, LC-ωBLYP fares little better in this regard than does LC-ωPBEsol or LC-ωLDA. While atomic energies are much better than they are for the other long-range-corrected hybrids investigated (but worse than those from BLYP itself), the heats of formation predicted by LC-ωBLYP are disappointingly poor. Additionally, unlike in BLYP, there is a large size-dependent error.

4.3. Barrier Heights. To more thoroughly assess performance for reaction barriers, we consider the HTBH38 set of 38 hydrogen-transfer barriers, and the NHTBH38 set of 38 non-hydrogen-transfer barriers. Results are presented in Table 4. Here, we see that, in all cases, semilocal functionals struggle to accurately describe reaction barriers, while the long-range-corrected hybrids are uniformly accurate. Part of this accuracy, admittedly, is due to ω being chosen with barrier heights emphasized, but a glance at Figure 3 shows that the range of ω over which long-range-corrected hybrids give reasonable barrier heights is rather broad. We note also that the errors in barrier heights are somewhat increased with LC-ωPBEsol and particularly with LC-ωLDA.

4.4. Ionization Potentials and Electron Affinites. We have thus far avoided any consideration of charged species. Since ions do play important roles in chemistry, it is worth considering performance of long-range-corrected hybrids for these cases. To assess performance of our long-range-corrected hybrids for charged species, we examine the G2 ion test set,[52] excluding N_2^+ and H_2S^+, which do not converge at the GGA level.[52] Our test set thus includes 86 ionization potentials (IPs) and 58 electron affinities (EAs). Results are calculated as the difference between the self-consistent energies of the neutral and charged species (in other words, these are "Δ-SCF" calculations). We report them in Table 5.

Table 5. Errors in Ionization Potentials (eV) and Electron Affinites (eV) for Several Long-Range-Corrected GGAs and for Their Parent GGAs[a]

	IP		EA	
model	ME	MAE	ME	MAE
LDA	0.05	0.23	0.23	0.24
PBEsol	−0.15	0.24	−0.08	0.21
PBE	−0.11	0.23	0.06	0.12
BLYP	−0.19	0.29	0.01	0.12
LC-ωLDA	0.64	0.64	0.46	0.46
LC-ωPBEsol	0.28	0.31	0.14	0.22
LC-ωPBE	0.07	0.19	0.02	0.18
LC-ωPBE08	0.11	0.20	0.02	0.19
LC-ωBLYP	−0.02	0.20	−0.03	0.18

[a] We show mean errors (ME) and mean absolute errors (MAE) for the 86 ionization potentials and 58 electron affinites of the G2 ion test set.

The principle result to which we should draw attention is that for neither IPs nor EAs does the long-range-correction improve upon the parent semilocal functional. That the semilocal functionals perform so well for electron affinites may be somewhat surprising, though it is documented in the literature. (See, for example, ref 50; note, however, that because we do not include plane waves in our basis set, these results may be somewhat artifactual.[53]) It is also perhaps somewhat surprising that LC-ωLDA fares so poorly for these compounds, even though the LSDA itself is not significantly worse than the GGAs we have examined. We note that while having the correct asymptotic decay of the exchange potential is critical if the ionization potential is to be evaluated from the highest occupied orbital energy, it is less important for ionization potentials evaluated in the Δ-SCF approach. We can of course evaluate the electron affinity from the ionization potential of the negatively charged species, and the same consideration would apply there.

5. Conclusions

Long-range-corrected hybrids offer some significant advantages, provided that they can be constructed. We feel that in constructing such a hybrid, one should make every effort to satisfy as many exact constraints as possible. By using the recently proposed GGA exchange hole model of ref 39, we can construct long-range-corrected hybrids from an exchange hole that obeys numerous exact constraints. Various GGAs differ only in the parameters used to define the function $\mathscr{H}(s)$, and once those parameters are determined for one's GGA of choice, the same code can be used for any long-range-corrected hybrid. Of course, which GGAs yield accurate long-range-corrected hybrids within this scheme is not known, but we can draw a few tentative conclusions. First, it does not seem to be particularly important which GGA is used in treating barrier heights of chemical reactions, though LC-ωLDA is notably poorer in this regard. The choice of GGA matters significantly more for atomic energies and for thermochemistry. Naturally, the proper range-separation parameter ω depends on the functional, and while we can draw no firm conclusions here, for the functionals we have considered, the optimal ω decreases as the gradient-dependence increases.

Acknowledgment. This work was supported by the National Science Foundation (Grant CHE-0807194) and the Welch Foundation (Grant C-0036). E.W. acknowledges additional support from the National Science Foundation and the U.S. Department of Defense (PHY-0755008).

Appendix A: Analytic Simplifications of the Range-Separated Enhancement Factor

We can identify several areas where numerical difficulties in evaluating the range-separated enhancement factor of eq 13 are likely to occur as ν becomes large. The polynomials in χ multiplying $\mathscr{B}/\lambda$, $\mathscr{CF}(s)/\lambda^2$, and $\mathscr{EG}(s)/\lambda^3$ all go to zero as ν goes to infinity. The logarithms vanish, and the remaining terms cancel up to order $1/\nu^2$. Here, we simplify the result in such a way as to be more numerically stable.

To simplify the polynomials in χ, we observe that

$$1-\chi=\frac{1-\chi^2}{1+\chi}=\frac{1}{1+\chi}\frac{\lambda}{\lambda+\nu^2}=\frac{\lambda}{\Lambda} \tag{23}$$

where this serves to define Λ. We note that, as $\nu\rightarrow 0$, $\Lambda\rightarrow\lambda$, while, as $\nu\rightarrow\infty$, $\Lambda\rightarrow 2\nu^2$.

To simplify the logarithms, we use, for example,

$$\begin{aligned}\frac{\nu+\sqrt{\zeta+\nu^2}}{\nu+\sqrt{\lambda+\nu^2}}&=1+\frac{\sqrt{\zeta+\nu^2}-\sqrt{\lambda+\nu^2}}{\nu+\sqrt{\lambda+\nu^2}}\\&=1+\frac{1}{\nu+\sqrt{\lambda+\nu^2}}\frac{\zeta-\lambda}{\sqrt{\zeta+\nu^2}+\sqrt{\lambda+\nu^2}}\end{aligned} \tag{24}$$

For large ν, this is $1+\mathscr{O}(1/\nu^2)$, and we can expand the logarithm in a power series.

We can simplify the remaining terms by noting that

$$\begin{aligned}2\nu\left(\sqrt{\zeta+\nu^2}-\sqrt{\eta+\nu^2}\right)&=\frac{2\nu(\zeta-\eta)}{\sqrt{\zeta+\nu^2}+\sqrt{\eta+\nu^2}}\\&=-\frac{2\nu\mathscr{A}}{\sqrt{\zeta+\nu^2}+\sqrt{\eta+\nu^2}}\end{aligned} \tag{25}$$

We thus have

$$\mathscr{A}+2\nu\left(\sqrt{\zeta+\nu^2}-\sqrt{\eta+\nu^2}\right)=\mathscr{A}\left(1-\frac{2\nu}{\sqrt{\zeta+\nu^2}+\sqrt{\eta+\nu^2}}\right) \tag{26a}$$

$$=\mathscr{A}\left(\frac{\zeta}{\left(\sqrt{\zeta+\nu^2}+\sqrt{\eta+\nu^2}\right)\left(\sqrt{\zeta+\nu^2}+\nu\right)}+\frac{\eta}{\left(\sqrt{\zeta+\nu^2}+\sqrt{\eta+\nu^2}\right)\left(\sqrt{\eta+\nu^2}+\nu\right)}\right) \tag{26b}$$

Putting it all together, a numerically more robust expression for the range-separated GGA enhancement factor is

$$\begin{aligned}F_{\mathrm{x}}^{\mathrm{SB}}(s,\nu)=\mathscr{A}&\left(\frac{\zeta}{\left(\sqrt{\zeta+\nu^2}+\sqrt{\eta+\nu^2}\right)\left(\sqrt{\zeta+\nu^2}+\nu\right)}+\frac{\eta}{\left(\sqrt{\zeta+\nu^2}+\sqrt{\eta+\nu^2}\right)\left(\sqrt{\eta+\nu^2}+\nu\right)}\right)-\frac{4}{9}\frac{\mathscr{B}}{\Lambda}-\\&\frac{4}{9}\frac{\mathscr{CF}(s)}{\Lambda^2}\left(1+\frac{1}{2}\chi\right)-\frac{8}{9}\frac{\mathscr{EG}(s)}{\Lambda^3}\left(1+\frac{9}{8}\chi+\frac{3}{8}\chi^2\right)+\\&2\zeta\ln\left(1-\frac{1}{\nu+\sqrt{\lambda+\nu^2}}\frac{\lambda-\zeta}{\sqrt{\lambda+\nu^2}+\sqrt{\zeta+\nu^2}}\right)-\\&2\eta\ln\left(1-\frac{1}{\nu+\sqrt{\lambda+\nu^2}}\frac{\lambda-\eta}{\sqrt{\lambda+\nu^2}+\sqrt{\eta+\nu^2}}\right)\end{aligned} \tag{27}$$

References

(1) Parr, R. G.; Yang, W. *Density Functional Theory of Atoms and Molecules*; Oxford University Press: New York, 1989.

(2) Dreizler, R. M.; Gross, E. K. U. *Density Functional Theory*; Plenum Press: New York, 1995.

(3) Scuseria, G. E.; Staroverov, V. N. Progress in the development of exchange-correlation functionals. In *Theory and Applications of Computational Chemistry: The First 40 Years*; Dykstra, C. E., Frenking, G., Kim, K. S., Scuseria, G. E., Eds.; Elsevier: Amsterdam, 2005.

(4) Levy, M. *Phys. Rev. A* **1982**, *26*, 1200.

(5) Lieb, E. H *Int. J. Quantum Chem.* **1983**, *24*, 243.

(6) Becke, A. D. *Phys. Rev. A* **1988**, *38*, 3098.

(7) Lee, C.; Yang, W.; Parr, R. G. *Phys. Rev. B* **1987**, *37*, 785.

(8) Perdew, J. P. In *Electronic Structure of Solids '91*; Ziesche, P., Eschrig, H., Eds.; Akademie Verlag: Berlin, 1991.

(9) Perdew, J. P.; Burke, K.; Ernzerhof, M. *Phys. Rev. Lett.* **1996**, *77*, 3865; **1997**, *E78*, 1396.

(10) Perdew, J. P.; Ruzsinszky, A.; Csonka, G. I.; Vydrov, O. A.; Scuseria, G. E.; Constantin, L. A.; Zhou, X.; Burke, K. *Phys. Rev. Lett.* **2008**, *100*, 136406.

(11) Voorhis, T. V.; Scuseria, G. E. *J. Chem. Phys.* **1998**, *109*, 400.

(12) Perdew, J. P.; Kurth, S.; Zupan, A.; Blaha, P. *Phys. Rev. Lett.* **1998**, *82*, 2544.

(13) Tao, J.; Perdew, J. P.; Staroverov, V. N.; Scuseria, G. E. *Phys. Rev. Lett.* **2003**, *91*, 146401.

(14) Zhao, Y.; Truhlar, D. G. *J. Chem. Phys.* **2006**, *125*, 194101.

(15) Becke, A. D. *J. Chem. Phys.* **1993**, *98*, 1372.

(16) Becke, A. D. *J. Chem. Phys.* **1993**, *98*, 5648.

(17) Stephens, P. J.; Devlin, F. J.; Chabalowski, C. F.; Frisch, M. J. *J. Phys. Chem.* **1994**, *98*, 11623.

(18) Ernzerhof, M.; Scuseria, G. E. *J. Chem. Phys.* **1999**, *110*, 5029.

(19) Adamo, C.; Barone, V. *J. Chem. Phys.* **1999**, *110*, 6158.

(20) Savin, A.; Flad, H.-J *Int. J. Quantum Chem.* **1995**, *56*, 327.

(21) Savin, A. On degeneracy, near-degenaracy and density functional theory In *Recent Developments and Applications of Modern Density Functional Theory*; Seminario, J. M., Ed.; Elsevier: Amsterdam, 1996.

(22) Leininger, T.; Stoll, H.; Werner, H.-J.; Savin, A. *Chem. Phys. Lett.* **1997**, *275*, 151.

(23) Monkhorst, H. J. *Phys. Rev. B* **1979**, *20*, 1504.

(24) Heyd, J.; Scuseria, G. E.; Ernzerhof, M. *J. Chem. Phys.* **2003**, *118*, 8207.

(25) Heyd, J.; Scuseria, G. E. *J. Chem. Phys.* **2004**, *120*, 7274.

(26) Heyd, J.; Scuseria, G. E. *J. Chem. Phys.* **2004**, *121*, 1187.

(27) Heyd, J.; Scuseria, G. E.; Ernzerhof, M. *J. Chem. Phys.* **2006**, *124*, 219906.

(28) Iikura, H.; Tsuneda, T.; Yanai, T.; Hirao, K. *J. Chem. Phys.* **2001**, *115*, 3540.

(29) Tawada, Y.; Tsuneda, T.; Yanagisawa, S.; Yanai, T.; Hirao, K. *J. Chem. Phys.* **2004**, *120*, 8425.

(30) Gerber, I. C.; Ángyán, J. G. *Chem. Phys. Lett.* **2005**, *415*, 100.

(31) Vydrov, O. A.; Scuseria, G. E. *J. Chem. Phys.* **2006**, *125*, 234109.

(32) Song, J.-W.; Hirosawa, T.; Tsuneda, T.; Hirao, K. *J. Chem. Phys.* **2007**, *126*, 154105.

(33) Chai, J.-D.; Head-Gordon, M. *J, Chem. Phys.* **2008**, *128*, 084106.

(34) Rohrdanz, M. A.; Herbert, J. M. *J. Chem. Phys.* **2008**, *129*, 034107.

(35) Sekino, H.; Maeda, Y.; Kamiya, M. *Mol. Phys.* **2005**, *103*, 2183.

(36) Henderson, T. M.; Izmaylov, A. F.; Scuseria, G. E.; Savin, A. *J. Chem. Phys.* **2007**, *127*, 221103.

(37) Henderson, T. M.; Izmaylov, A. F.; Scuseria, G. E.; Savin, A. *J. Chem. Theory. Comput.* **2008**, *4*, 1254.

(38) Ernzerhof, M.; Perdew, J. P. *J. Chem. Phys.* **1998**, *109*, 3313.

(39) Henderson, T. M.; Janesko, B. G.; Scuseria, G. E. *J. Chem. Phys.* **2008**, *128*, 194105.

(40) Antoniewicz, P. R.; Kleinman, L. *Phys. Rev. B* **1985**, *31*, 6779.

(41) Lynch, B. J.; Truhlar, D. G. *J. Phys. Chem. A* **2003**, *107*, 8996; **2004**, *E108*, 1460.

(42) Pople, J. A.; Head-Gordon, M.; Fox, D. J.; Raghavachari, K.; Curtiss, L. A. *J. Chem. Phys.* **1989**, *90*, 5622.

(43) Curtiss, L. A.; Jones, C.; Trucks, G. W.; Raghavachari, K.; Pople, J. A. *J. Chem. Phys.* **1990**, *93*, 2537.

(44) Curtiss, L. A.; Raghavachari, K.; Redfern, P. C.; Pople, J. A. *J. Chem. Phys.* **1997**, *106*, 1063.

(45) Curtiss, L. A.; Raghavachari, K.; Redfern, P. C.; Pople, J. A. *J. Chem. Phys.* **2000**, *112*, 7374.

(46) Zhao, Y.; Lynch, B. J.; Truhlar, D. G. *Phys. Chem. Chem. Phys.* **2004**, *7*, 43.

(47) Zhao, Y.; González-García, N.; Truhlar, D. G. *J. Phys. Chem. A* **2005**, *109*, 2012; **2006**, *110*, 4942(E).

(48) Chakravorty, S. J.; Gwaltney, S. R.; Davidson, E. R.; Parpia, F. A.; Fischer, C. F. *Phys. Rev. A* **1993**, *47*, 3649.

(49) Vydrov, O. A.; Heyd, J.; Krukau, A. V.; Scuseria, G. E. *J. Chem. Phys.* **2006**, *125*, 074106.

(50) Staroverov, V. N.; Scuseria, G. E.; Tao, J.; Perdew, J. P. *J. Chem. Phys.* **2003**, *119*, 12129.

(51) Brothers, E. N.; Scuseria, G. E. *J. Chem. Theory Comput.* **2006**, *4*, 1045.

(52) Curtiss, L. A.; Redfern, P. C.; Raghavachari, K.; Pople, J. A. *J. Chem. Phys.* **1998**, *109*, 42.

(53) Rösch, N.; Trickey, S. B. *J. Chem. Phys.* **1996**, *106*, 8940.

CT800530U